Monthly Notices
of the
ROYAL ASTRONOMICAL SOCIETY

MNRAS **456,** 2717–2721 (2016) doi:10.1093/mnras/stv2851

Swift reveals the eclipsing nature of the high-mass X-ray binary IGR J16195−4945

G. Cusumano,★ V. La Parola,★ A. Segreto and A. D'Aì
INAF, Istituto di Astrofisica Spaziale e Fisica Cosmica, Via U. La Malfa 153, I-90146 Palermo, Italy

Accepted 2015 December 2. Received 2015 November 30; in original form 2015 October 12

ABSTRACT

IGR J16195−4945 is a hard X-ray source discovered by *INTEGRAL* during the Core Programme observations performed in 2003. We analysed the X-ray emission of this source exploiting the *Swift*-Burst Alert Telescope (BAT) survey data from 2004 December to 2015 March, and all the available *Swift*-X-ray Telescope (XRT)-pointed observations. The source is detected at a high significance level in the 123-month BAT survey data, with an average 15–150 keV flux of the source of ∼1.6 mCrab. The timing analysis on the BAT data reveals with a significance higher than six standard deviations the presence of a modulated signal with a period of 3.945 d, that we interpret as the orbital period of the binary system. The folded light curve shows a flat profile with a narrow full eclipse lasting ∼3.5 per cent of the orbital period. We requested phase-constrained XRT observations to obtain a more detailed characterization of the eclipse in the soft X-ray range. Adopting reasonable guess values for the mass and radius of the companion star, we derive a semimajor orbital axis of $\sim 31\,R_{\odot}$, equivalent to ∼1.8 times the radius of the companion star. From these estimates and from the duration of the eclipse, we derive an orbital inclination between 55 and 60 deg. The broad-band time-averaged XRT+BAT spectrum is well modelled with a strongly absorbed flat power law, with absorbing column $N_{\rm H} = 7 \times 10^{22}\,{\rm cm}^{-2}$ and photon index $\Gamma = 0.5$, modified by a high energy exponential cutoff at $E_{\rm cut} = 14$ keV.

Key words: binaries: eclipsing – X-rays: binaries – X-rays: individual: IGR J16195−4945.

1 INTRODUCTION

Thanks to the imaging capability of the Burst Alert Telescope (BAT; Barthelmy et al. 2005) on board of the *Swift* observatory (Gehrels et al. 2004) we have an all-sky, nearly continuous in time and spatially resolved monitoring in the 15–150 keV energy band since 2004 December. BAT observes daily ∼90 per cent of the sky thanks to its very large field of view (1.4 steradian half coded) and to the pointing strategy of the *Swift* observatory that performs tens of pointings per day towards different directions of the sky. This huge data set has proved extremely useful for spectral and temporal studies of numerous Galactic and extragalactic sources.

In this paper, we exploit the hard X-ray monitoring collected by BAT on IGR J16195−4945. We assess the binary nature of the source through the detection of its orbital period and derive information on the geometry of the system. Moreover, broad-band spectral analysis is performed using also the soft X-ray data collected by the X-ray Telescope (XRT; Burrows et al. 2005) during the pointed observations performed by *Swift*.

★E-mail: cusumano@ifc.inaf.it (GC); laparola@ifc.inaf.it (VLP)

IGR J16195−4945 is a faint source discovered by *INTEGRAL* during the Core Program observations performed between 2003 February 27 and October 19 (Walter et al. 2004). The source was detected in the direction of the Norma region of the Galaxy ($332^{\circ} < l < 334^{\circ}$, at ∼5 kpc; Russeil 2003). In the fourth IBIS/ISGRI catalogue (Bird et al. 2010) IGR J16195−4945 is reported with an intensity of ∼2.0 and ∼1.2 mCrab in the energy ranges 20–40 keV and 40–100 keV, respectively.

Sidoli et al. (2005) proposed the *ASCA* X-ray source AX J161929−4945 as the likely soft X-ray counterpart of this source. The analysis of archival *ASCA* observations showed a variable flux with a variation of the source intensity up to a factor of ∼2.5. The *ASCA* spectrum of the source was modelled by an absorbed power law with a photon index of ∼0.6, a high value of $N_{\rm H} \sim 12 \times 10^{22}\,{\rm cm}^{-2}$ and an observed flux of $1.6 \times 10^{-11}\,{\rm erg\,cm}^{-2}\,{\rm s}^{-1}$ in 2–10 keV. Analysing archival *INTEGRAL* data, Sidoli et al. (2005) detected IGR J16195−4945 in only two observations out of 56 (2003 March 4 and 14) both with an average flux level of ∼17 mCrab in the 20–40 keV range.

During an *INTEGRAL* observation performed on 2003 September 26, the source showed a flare lasting ∼1.5 h reaching a peak flux of ∼35 mCrab in 20–40 keV (Sguera et al. 2006). Because of

the time-scale of the event, the source was classified as a possible Supergiant Fast X-ray Transient (SFXT) candidate.

Chandra observed the source on 2005 April 29 allowing us to refine its position at RA = $16^{h}19^{m}32\overset{s}{.}20$, Dec. = $-49^{\circ}44'30\overset{''}{.}7$ (J2000), with an accuracy of 0.6 arcsec (Tomsick et al. 2006). This in turn allowed us to find the nIR and mIR counterparts in the Two Micron All-Sky Survey (2MASS J16193220−4944305) and in the Galactic Legacy Infrared Mid-Plane Survey Extraordinaire (G333.5571 + 00.3390) catalogues, respectively. The *Chandra* spectrum was best fitted by an absorbed power law (Gamma ∼0.5 and $N_{\rm H} \sim 7 \times 10^{22}$ cm^{-2}, unabsorbed flux of 4.6×12^{-12} erg cm^{-2} s^{-1} in the 0.3–10 keV range). Extracting a time-averaged spectrum using all the available public *INTEGRAL* data from 2003 February 27 to 2004 September 15, Tomsick et al. (2006) found a best-fitting power law with photon index ∼1.7 and a 20–50 kev flux of 19×10^{-12} erg cm^{-2} s^{-1}. Assuming that the source is in the Norma-Cygnus arm of the Galaxy and thus at a distance of 5 kpc, the derived X-ray luminosities are 1.4×10^{34} (d/5 kpc)^2 erg s^{-1} in the 0.3–10 keV range and 5.8×10^{34} (d/5 kpc)^2 erg s^{-1} in the 20–50 keV range. The nature of the companion star was constrained through the analysis of photometric and spectroscopic data in the optical and near-infrared band, that allowed the identification of the spectral type of the companion star as an ON9.7Iab supergiant star (Coleiro et al. 2013).

IGR J16318−4848 was observed by *Suzaku* in 2006 September. During this observation IGR J16195−4945 showed a short (∼5000 s) bright flare (∼10 × brighter than the prior emission level) adding evidence for its SFXT nature (Morris et al. 2009). The emission during the flare was modelled by an absorbed power law and a partial covering model with a photon index of ∼1.8 and an average flux of 4.8×10^{-11} erg cm^{-2} s^{-1} in the 0.2–10 keV range. If IGR J16195−4945 is a SFXT and assuming the equatorial disc wind model (Sidoli et al. 2007), that interprets the observed bright flare as the transit of the compact object into an equatorial disc wind of the donor star, and combining *Suzaku* data with the long-term *Swift*-BAT data set, Morris et al. (2009) predicted for this source an orbital period of ∼16 d.

This paper is organized as follows. Section 2 describes the data reduction. Section 3 reports on the timing analysis. In Section 4, we describe the spectral analysis and in Section 5 we briefly discuss our results.

2 DATA REDUCTION

The BAT survey data collected between 2004 December and 2015 March were retrieved from the HEASARC public archive[1] and processed with the BAT_IMAGER code (Segreto et al. 2010), a software built for the analysis of data from coded mask instruments that performs screening, mosaicking and source detection, and produces scientific products of any revealed source.

IGR J16195−4945 was detected in the 15–150 keV band at a significance of 28.5 standard deviations, with a maximum of significance (31.7 standard deviations) in the 15–60 keV energy band. Fig. 1 shows the 15–60 keV significance sky map (exposure time of 44.1 ms) centred in the direction of IGR J16195−4945. For the timing analysis of the BAT data, we extracted the light curve in the 15–60 keV energy range with the maximum available time resolution of ∼300 s while for the spectral analysis, we produced the background subtracted spectrum of the source averaged over the entire exposure and we used the official BAT spectral redistribution matrix[2]

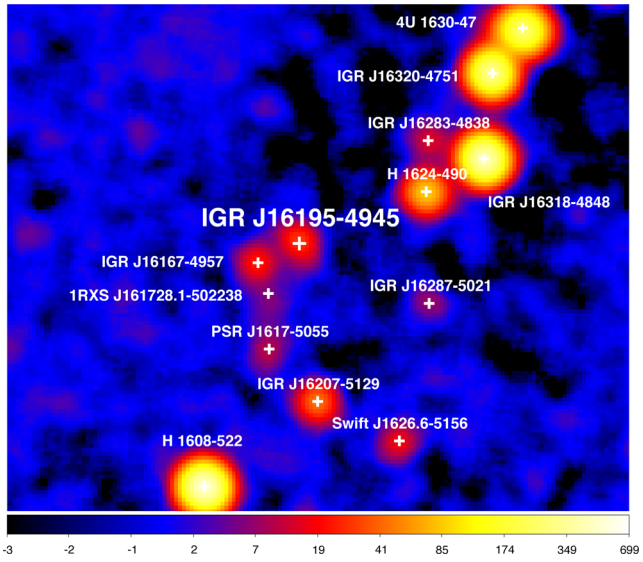

Figure 1. Left-hand panel: 15–60 keV significance map in the neighbourhood of IGR J16195−4945.

We have analysed all the available *Swift*-XRT observations of IGR J16195−4945. The source was always observed in photon counting (PC) mode. In Table 1, we show the log of the *Swift*-XRT observations and the relevant source count rates. The XRT data were processed with standard procedures (XRTPIPELINE v.0.12.4), filtering and screening criteria, using ftools in the HEASOFT package (v 6.12), adopting standard grade filtering 0–12. The event arrival times were reported to the Solar system Barycentre using the task BARYCORR.[3] For each observation, we extracted the source data from a circular region of 20 pixel radius (1 pixel = 2.36 arcsec) centred on the source position as determined with XRTCENTROID.[4] The spectra were rebinned with a minimum of 20 counts per energy channel. This lower limit of counts per bin is enough to ensure that the deviation of the observed number of counts from the expected values approximates quite well a Gaussian distribution, that is a requirement to apply the χ^2 statistics. The background was extracted from an annular region centred on the source with radii of 70 and 130 pixels. XRT ancillary response files were generated with XRTMKARF[5]

We used the spectral redistribution matrix v014 and the spectral analysis was performed using XSPEC v.12.5. Errors are at 90 per cent confidence level, if not stated otherwise.

3 TIMING ANALYSIS

We analysed the long-term BAT light curve searching for any periodic signal. The 15–60 keV BAT light curve was folded with different trial periods P from 1.0 d to 500 d with a step of $P^2/(N\,\Delta T)$, where $N = 16$ is the number of trial profile phase bins and $\Delta T \sim 323$ ms is the data span length. To build the profile for each trial period the average rate in each phase bin was evaluated by weighting the rates with the inverse square of their statistical error.

[1] http://heasarc.gsfc.nasa.gov/docs/archive.html

[2] http://heasarc.gsfc.nasa.gov/docs/heasarc/caldb/data/swift/bat/index.html
[3] http://heasarc.gsfc.nasa.gov/ftools/caldb/help/barycorr.html
[4] http://heasarc.gsfc.nasa.gov/ftools/caldb/help/xrtcentroid.html
[5] http://heasarc.gsfc.nasa.gov/ftools/caldb/help/xrtmkarf.html

Table 1. Log of the *Swift*-XRT observations.

Obs #	Obs ID	$T_{\rm start}$ (MJD)	$T_{\rm elapsed}$ (s)	Exposure (s) (s)	Rate (c/s)$\times 10^{-2}$	Orb. phase
1	00036628001	54385.749	104 580	9055	12.4 ± 0.5	0.435–0.742
2	00038000001	54654.040	59 057	7561	10.8 ± 0.5	0.442–0.616
3	00038000002	55350.107	29 625	3646	1.4 ± 0.3	0.885–0.972
4	00042873001	56079.489	469	469	33.0 ± 0.4	0.773–0.774
5	00042866001	56079.892	484	484	7.9 ± 1.9	0.875–0.876
6	00042866002	56081.497	266	266	2.7 ± 1.4	0.282–0.283
7	00649143000	57219.140	1321	1316	1.5 ± 0.5	0.658–0.662
8	00649143001	57219.206	6260	2170	2.8 ± 0.5	0.675–0.693
9	00037887001	57295.035	659	659	0.8 ± 0.5	0.895–0.897
10	00037887002	57295.102	522	522	0.7 ± 0.5	0.913–0.914
11	00037887003	57295.164	742	742	<1.48	0.928–0.930
12	00037887004	57295.230	577	577	<3.24	0.945–0.946
13	00037887005	57295.297	504	504	<3.05	0.962–0.964
14	00037887006	57295.367	637	637	<1.78	0.980–0.982
15	00037887007	57295.434	509	509	<2.24	0.997–0.998
16	00037887008	57295.496	527	527	<2.15	0.013–0.014
17	00037887009	57295.563	557	557	<2.05	0.029–0.031
18	00037887010	57295.637	612	612	<1.85	0.048–0.049
19	00037887011	57295.699	539	539	<3.48	0.064–0.066
20	00037887012	57295.766	452	452	<3.40	0.081–0.082
21	00037887013	57295.840	492	492	8.5 ± 1.7	0.099–0.101
22	00037887014	57295.906	552	552	5.7 ± 1.4	0.116–0.118
23	00037887015	57295.965	384	384	4.1 ± 1.4	0.132–0.133

This procedure is mandatory for data collected by a large field of view coded mask telescope like BAT that is characterized by a large spread of statistical count rate errors. Fig. 2 (Top panel) shows the resulting periodogram, where a single feature emerges, reaching a χ^2 value of ∼116, at a period of $P_0 = 3.945 \pm 0.005$ d, where P_0 and its error are the centroid and the standard deviation obtained by modelling this feature with a Gaussian function. We observe that in a wide interval of trial periods (1–50 d) around the feature position the average χ^2 is ∼20, and therefore it deviates significantly from the average value of $N-1$ expected for the χ^2 statistics for a white noise signal. As a consequence, to estimate the significance of P_0, we applied the method described in Segreto et al. (2013), obtaining that the probability of finding a value of χ^2 equal or higher than 116 is 1.8×10^{-10}, corresponding to more than six standard deviations in Gaussian statistics.

The BAT light curve folded at P_0 with $T_{\rm epoch} = 55220.4179$ MJD shows a quite flat intensity level and a sharp dip consistent with no emission. To evaluate the phase position of the dip centroid, we built a new profile, adopting a finer ($N = 30$) phase bin grid (Fig 2, central panel) and fitted the dip with a Gaussian model: the centroid is at phase 0.02 ± 0.01 corresponding to $(55220.50 \pm 0.04) \pm nP_0$ MJD, while the full width at half-maximum (FWHM) is 0.08 ± 0.02 in phase, corresponding to 0.32 ± 0.07 d. To confirm the presence of the dip in the soft X-ray band, we requested a *Swift*-XRT monitoring of the source in the phase interval around the dip (Obs # 9–23 in Table 1, corresponding to orbital phases 0.91–1.13). Fig. 3 shows the XRT count rates of all the XRT observations folded at P_0. The shaded area corresponds to the phase interval of the BAT dip. In all the observations within the dip phase interval the source is not detected, strongly suggesting an eclipse of the compact source by the companion star. Cumulating observations 11 to 20, we obtain a more stringent upper limit to the source count rate of 2.4×10^{-3} count s^{-1}.

Where the source is detected, its count rate shows significant variability, with a variation of a factor of ∼30 between the two

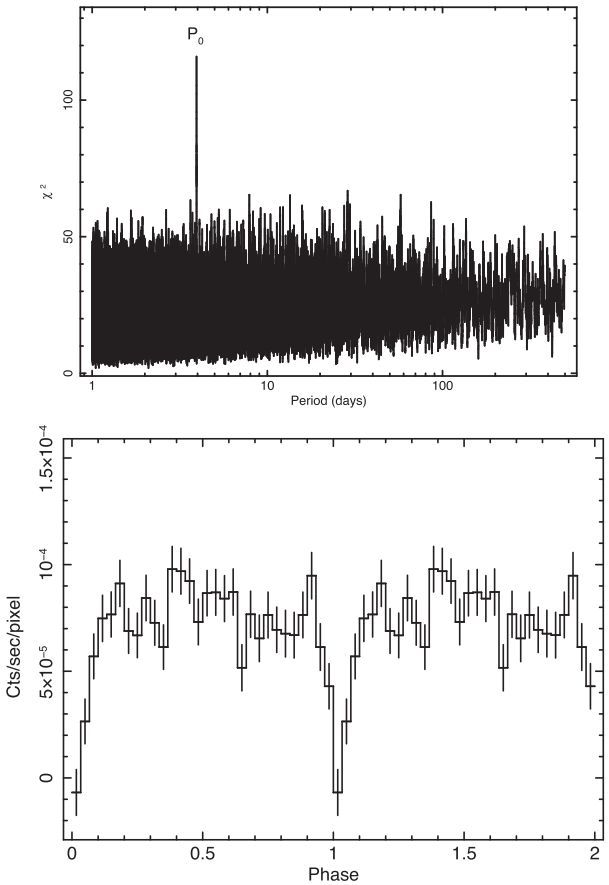

Figure 2. Top panel: periodogram of *Swift*/BAT (15–60 keV) data for IGR J16195−4945. Bottom panel: light curve folded at a period $P = 3.945$ d, with 30 phase bins.

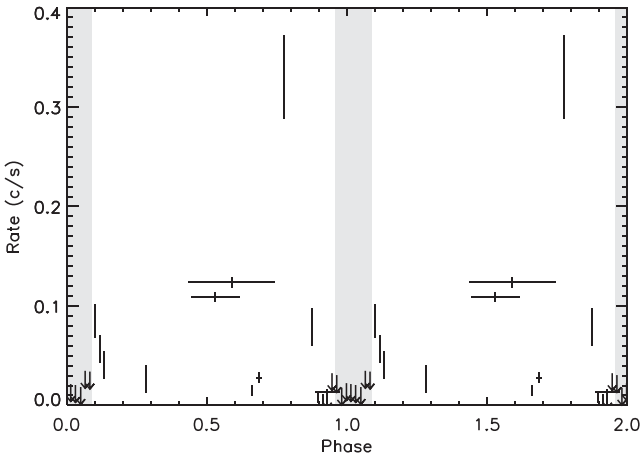

Figure 3. XRT count rate of the pointed observations versus orbital phase. The shaded area is centred on the minimum in the BAT folded light curve and its width is FWHM of the Gaussian that best fit the dip.

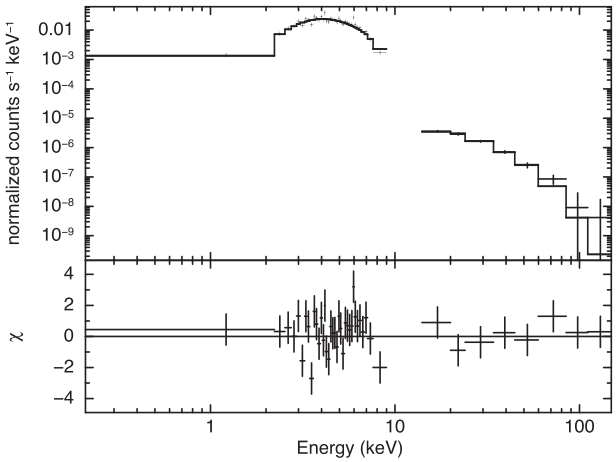

Figure 4. Top panel: IGR J16195−4945 spectrum (XRT+BAT) and best-fitting model. Bottom panel: residuals in unit of standard deviations.

observations with extreme rate values (Obs 4 and 10). An inspection of the light curves extracted from each observation shows a rate variation of a factor of <5 within each data set.

We performed a search for periodic modulations only on the XRT data from observations 1 and 2, as the statistics of the other data sets is too low for this kind of analysis. In order to avoid systematics caused by the read-out time in PC mode characterized by a time resolution bin of $\delta T_{\rm XRT} = 2.5073$ s, the arrival times of the events in PC mode were randomized within $\delta T_{\rm XRT}$. We performed a folding analysis on the source data from each observation searching in the period range between $\delta T_{\rm XRT}$ and 1000 s. We did not find any significant feature in the resulting periodograms.

4 BROAD-BAND SPECTRAL ANALYSIS

We performed a broad-band spectral analysis in the 0.2–150 keV energy range. We used only the XRT data extracted from observations 1 and 2; the other XRT observations were not used because of their low statistics. A preliminary analysis showed no significant differences between the two spectra, and they were therefore summed into a single spectrum. We also checked for the presence of any significant spectral variability during the BAT monitoring through the inspection of the hardness ratio calculated in the energy ranges [35–85 keV][15–35 keV] with several time bins between 1 and 20 d. We found no significant variability on any time-scale.

Therefore, we performed the broad-band spectral analysis coupling the soft X-ray spectrum with the BAT spectrum averaged over 123 months, adding a constant factor to take into account both an intercalibration factor between the two telescopes and the different flux level between the two data sets. An absorbed power-law model gave an unacceptable χ^2 of 165 with 76 d.o.f., with evident residuals between the data and the best-fitting model. The spectra indeed resulted well fitted ($\chi^2 = 80.0$ with 75 d.o.f.) using a power law with a cutoff at ∼14 keV absorbed by a column of $N_{\rm H} = (7 \pm 1) \times 10^{22}$ cm^{-2} (model `tbabs*(cutoffpl)` in XSPEC).

Fig. 4 shows the combined XRT and BAT spectral data with the best-fitting model (top panel) and the residuals in unit of standard deviations (bottom panel). Table 2 reports the best-fitting parameters.

Table 2. Best-fitting spectral parameters. We report unabsorbed fluxes for the characteristic XRT (0.2–10 keV) and BAT (15–150 keV) energy bands.

Parameter	Best-fitting value	Units
$N_{\rm H}$	$7.0^{+1.3}_{-1.1} \times 10^{22}$	cm^{-2}
Γ	$0.5^{+0.3}_{-0.3}$	
$E_{\rm cut}$	14^{+3}_{-2}	keV
N	$(1.3^{+0.9}_{-0.5}) \times 10^{-3}$	ph keV^{-1}cm^{-2}s^{-1} at 1 keV
$C_{\rm BAT}$	$0.49^{+0.14}_{-0.11}$	
F (0.2–10 keV)	$(2.7 \pm 0.3) \times 10^{-11}$	erg s^{-1} cm^{-2}
F (15–150 keV)	$(2.2 \pm 0.2 \times 10^{-11}$	erg s^{-1} cm^{-2}
χ^2	80.1 (75 d.o.f.)	

5 DISCUSSION

In this paper, we have exploited the *Swift* archival data set on IGR J16195−4945. The source is detected at a level of 28.5 standard deviations cumulating the first 123 months of BAT survey data, with an average flux of $(2.2 \pm 0.2) \times 10^{-11}$ erg s^{-1} cm^{-2} in the 15–150 keV band, corresponding to $(6.5 \pm 0.6) \times 10^{34}$ erg s^{-1} assuming a distance of 5 kpc. The intrinsic flux in the soft X-ray band (0.2–10 keV) ranges between 0.3×10^{-11} erg s^{-1} cm^{-2} and 6.2×10^{-11} erg cm^{-2} s^{-1}, corresponding to a luminosity of 8.9×10^{33} erg s^{-1} and 1.8×10^{35} erg s^{-1}, respectively. We have performed a broad-band 15–150 keV spectral analysis combining the XRT and BAT average spectra. The source spectrum is well modelled with an absorbed power law with a cutoff at ∼14 keV. The column density and the power-law slope are $\sim 7 \times 10^{22}$ cm^{-2} and ∼0.5, respectively, in full agreement with the values observed with *Chandra* (Tomsick et al. 2006). This spectral shape is typical for high-mass X-ray binary pulsars (Coburn et al. 2002).

The timing analysis performed on the BAT light curve reveals the presence of a modulated signal with a periodicity $P_0 = 3.945 \pm 0.005$ d, that we interpret as the orbital period of this binary system. Using indicatively the same mass and radius derived for the O9.7-type companion star in the Cyg X−1 system ($M_\star \sim 24\,{\rm M}_\odot$ and $R_\star \sim 17\,{\rm R}_\odot$, respectively; Ziółkowski 2014), we can derive the semimajor axis of the system through the application of the Kepler's third law:

$$a = (G P_0^2 (M_\star + M_{\rm X})/4\pi^2)^{1/3} \simeq 31\,{\rm R}_\odot \simeq 1.8 R_\star, \quad (1)$$

if we assume the compact object to be a neutron star with $M_X = 1.4\,M_\odot$. The BAT light curve folded with a period of P_0 shows a flat profile interrupted by a full eclipse with estimated mid-eclipse time of MJD $(55220.50 \pm 0.04) \pm nP_0$. The monitoring of *Swift*-XRT shows that the source is not detected during the eclipse phase interval, with a 3σ upper limit of 4.4×10^{-13} erg cm^{-2} s^{-1}, while it is always well visible outside this interval. The full eclipse lasts ∼3.5 per cent of the orbital period (∼0.14 d): such a short duration corresponds to an inclination of the orbit between 55 and 60 deg, under the hypothesis that the orbit has a very low eccentricity, as the flatness of the folded light curve suggests.

We have analysed the long-term *Swift*-BAT light curve of the source IGR J16195−4945 to study its variability. The source light curve in the 15–60 keV band (where the source has the highest significance) was binned into 1, 2, 6, 12 h intervals in order to examine the source behaviour on these time-scales. The average intensity level of the source is ∼1.6 mCrab. The most significant deviations from this average level (with an S/N ratio of >5) reach an intensity of ∼50 mCrab on hours time-scale, and ∼15 mCrab with a time bin of 12 h. However, the overall distribution of the observed S/N values in the relevant light curves shows that the significance values of these peaks are only marginal outliers with respect to the observed fluctuations. We conclude that short time flares of the order of tenth of mCrab (such as those observed with other satellites; Sguera et al. 2006; Morris et al. 2009) cannot be revealed with the sensitivity of the BAT light curves. On the other hand, the pointed XRT observations outside the eclipse, although did not show any clear flaring episode within a single observation, differ in the observed averaged count rates up to a factor of 20. Assuming the best-fitting broad-band spectral model (table 4), the two extreme XRT count rate values, extrapolated to the 15–60 keV band, correspond to 0.36 and 7.6 mCrab, respectively.

ACKNOWLEDGEMENTS

This work was supported in Italy by ASI contract I/004/11/1. We thank the *Swift* team for having promptly performed the ToO observations analysed in this paper.

Facility: *Swift*.

REFERENCES

Barthelmy S. D. et al., 2005, Space Sci. Rev., 120, 143
Bird A. J. et al., 2010, ApJS, 186, 1
Burrows D. N. et al., 2005, Space Sci. Rev., 120, 165
Coburn W., Heindl W. A., Rothschild R. E., Gruber D. E., Kreykenbohm I., Wilms J., Kretschmar P., Staubert R., 2002, ApJ, 580, 394
Coleiro A., Chaty S., Zurita Heras J. A., Rahoui F., Tomsick J. A., 2013, A&A, 560, A108
Gehrels N. et al., 2004, ApJ, 611, 1005
Morris D. C., Smith R. K., Markwardt C. B., Mushotzky R. F., Tueller J., Kallman T. R., Dhuga K. S., 2009, ApJ, 699, 892
Russeil D., 2003, A&A, 397, 133
Segreto A., Cusumano G., Ferrigno C., La Parola V., Mangano V., Mineo T., Romano P., 2010, A&A, 510, A47
Segreto A., Cusumano G., La Parola V., D'Aì A., Masetti N., D'Avanzo P., 2013, A&A, 557, A113
Sguera V. et al., 2006, ApJ, 646, 452
Sidoli L., Vercellone S., Mereghetti S., Tavani M., 2005, A&A, 429, L47
Sidoli L., Romano P., Mereghetti S., Paizis A., Vercellone S., Mangano V., Götz D., 2007, A&A, 476, 1307
Tomsick J. A., Chaty S., Rodriguez J., Foschini L., Walter R., Kaaret P., 2006, ApJ, 647, 1309
Walter R. et al., 2004, Astron .Telegram, 229, 1
Ziółkowski J., 2014, MNRAS, 440, L61

This paper has been typeset from a TEX/LATEX file prepared by the author.